Natalia E. Chubarova[1]*, **Elizaveta E. Androsova[1]**, **Alexandr A. Kirsanov[2]**, **Bernhard Vogel[4]**, **Heike Vogel[4]**, **Olga B. Popovicheva[3]**, **Gdali S. Rivin[2,1]**

[1] Moscow State University, Faculty of Geography, 119991, Moscow, Russian Federation
[2] Hydrometeorological Centre of Russia, 11-13, B. Predtechensky per., Moscow, 123242, Russia
[3] Moscow State University, Faculty of Physics, 119991, P.O. Box 3640 76021, Moscow, Russian Federation
[4] Karlsruhe Institute of Technology, Karlsruhe, Germany
***Corresponding author:** natalia.chubarova@gmail.com

AEROSOL AND ITS RADIATIVE EFFECTS DURING THE AERORADCITY 2018 MOSCOW EXPERIMENT

ABSTRACT. During the AeroRadCity-2018 spring aerosol experiment at the Moscow State University Meteorological Observatory the aerosol properties of the atmosphere and radiative aerosol effects were analyzed using a wide complex of measurements and model COSMO-ART simulations over Moscow domain. The program of measurements consisted of columnar aerosol AERONET retrievals, surface PM10, black carbon (BC) and aerosol gas precursors mass concentrations, as well as radiative measurements under various meteorological conditions. We obtained a positive statistically significant dependence of total and fine aerosol optical depth (AOD) mode (R^2~0.4) with PM concentrations. This dependence has revealed a pronounced bifurcation point around PM10=0.04 mgm^{-3}. The modelled BC concentration is in agreement with the observations and has a pronounced correlation with PM, but not with the AODs. The analysis of radiative effects of aerosol has revealed up to 30% loss for UV irradiance and 15% - for shortwave irradiance at high AOD in Moscow. Much intensive radiation attenuation is observed in the afternoon when remote pollution sources may affect solar fluxes at elevated boundary layer conditions. Negative (cooling) radiative forcing effect at the top of the atmosphere from -18 Wm^{-2} to -4 Wm^{-2} has been evaluated. Mean difference in visible AOD between urban and background conditions in Moscow and Zvenigorod was about 0.01 according to measurements and model simulations, while in some days the difference may increase up to 0.05. The generation of urban aerosol was shown to be more favorable in conditions with low intensity of pollutant dispersion, when mean deltaAOD550 was doubled from 0.01 to 0.02.

KEY WORDS: surface and columnar aerosol, black carbon, COSMO-ART, radiation, urban aerosol pollution, AERONET

INTRODUCTION

Atmospheric aerosol has a complex effect on the biosphere. It significantly affects the properties of the atmosphere, providing the uncertainty of climate change and directly affects human health increasing premature mortality and reduction of life (IPCC 2013; http://www.who.int/mediacentre/factsheets/fs313/en/). Depending on its optical and microphysical properties due to the processes of absorption and scattering of solar radiation, as well as through direct interaction with the cloud elements, the aerosol has different effects on temperature and humidity conditions of the atmosphere, thus determining the quality of the weather forecast and influencing regional climate. All these processes are exacerbated in the urban environment, where aerosol concentrations significantly increased and their optical properties changed dramatically. However, the estimates of the aerosol effects have large uncertainty, especially in the urban environment (Tegen et al. 1997; IPCC 2013). One of the most important components of an urban aerosol is black carbon (BC), a short-lived climate tracer, which stands on the second place in contributing atmospheric warming after carbon dioxide (IPCC 2013). Due to its properties BC significantly absorbs visible irradiance thus significantly affecting net shortwave radiation. Detailed studies of BC were carried out in IAP RAS (Kopeikin 1998; Golitsyn et al. 2015), in Western Siberia (Kozlov et al. 2016). There are several approaches (see, for example, Kozlov et al. 2008), in which BC measurements are used for retrieving aerosol single scattering albedo, which is one of the important aerosol parameters for radiative transfer (RT) modelling.

Different chemical, photochemical and meteorological processes play an important role in the urban aerosol formation affecting total columnar aerosol and, hence, further influencing the radiative and meteorological characteristics (Vogel et al. 2009, Chubarova et al. 2018). However, there are still gaps in understanding the reasons of various types of relationships between ground-based and columnar aerosol content. In addition, urban aerosol can change the absorbing properties of the atmosphere of large megacities (see for, example, Chubarova et al, 2011b). For studying these effects mesoscale atmospheric models with good temporal and spatial resolution can be used. One of them is the COSMO (COnsortium for Small-scale MOdelling) mesoscale model (http://www.cosmo-model.org/), which is currently an operational weather prediction model at the Hydrometeorological Centre of Russia. The ART (Aerosols and Reactive Trace gases) chemical model as a part of COSMO model (Vogel et al. 2010) allows a user to simulate the formation of secondary aerosol and gives the opportunity to quantify the rate of formation of new particles in the polluted urban atmosphere under different atmospheric conditions.

For understanding the physical processes of generating different aerosol types and their effects on solar irradiance, an intensive measurement campaign (AeroRadCity) has been carried out in spring 2018 at the Meteorological Observatory (MO), of Moscow State University. The AeroRadCity-2018 experiment included both experimental and model aerosol and radiation studies for better understanding the role of a large megacity in generating urban aerosol and evaluating its effects on solar irradiance.

In this paper we focus on the following tasks:

• Identification of the relationship between meteorological conditions with an additional characterization of the intensity of the particle dispersion (IPD) and different aerosol characteristics for quantifying the relation between surface and columnar aerosol loading.

• Evaluation of the aerosol radiative effects in different spectral regions.

• Assessment of the urban component of aerosol.

We analyze spring conditions since within a relatively short period we could test all

situations typical both for cold and warm seasons including important biomass burning episodes for studying a wide variety of different aerosol properties and their effects on solar radiation.

MATERIALS AND METHODS

The AeroRadCity-2018 experiment observational campaign included a large complex of measurements of different surface and columnar aerosol properties, aerosol gas precursors, as well as radiative and meteorological parameters at the Meteorological Observatory of Moscow State University (MO MSU), (55.707°N, 37.522°E, http://momsu.ru/english.html), which is located at the territory of the MSU Botanical Garden in the area of Vorobyovy Gory (Vorobyovy hills) far from local emission sources. MO MSU is qualified as an urban background site (Chubarova et al. 2014). The complex of aerosol measurements consisted of columnar aerosol characteristics from sun/sky CIMEL photometer installed at the MO MSU roof as a part of the AERONET program (Holben et al. 1998; Chubarova et al. 2011a). The AERONET aerosol retrievals included aerosol optical depth (AOD) within the spectral range from 340 nm to 1020 nm, Angstrom exponent, fine and coarse aerosol AOD modes at 500nm according to the retrieval method described in (O'Neill et al. 2001), single scattering albedo (SSA) and aerosol factor of asymmetry (ASYM) according to Dubovik and King (2000). The measurements of columnar aerosol characteristics were made in clear solar disk conditions using the additional cloud-screening filter described in (Chubarova et al. 2016). The data from the latest version 3 with final instrument calibration (level 2) were used for Moscow, and the data from version 3 at level 1.5– for Zvenigorod site, since no final data calibration is still available there. However, according to the experience, the correction usually does not exceed 0.01 AOD in a visible spectral region.

Setup of instruments for real-time equivalent black carbon mass concentration measurements and PM sampling was also installed at the MO MSU roof. Aerosol equivalent BC concentrations (marked as BC) were measured using the portable aethalometer developed by the MSU/CAO group (Popovicheva et al. 2019). In this instrument, the light attenuation caused by the particles depositing on a quartz fiber was measured at three wavelengths (450, 550, and 650 nm). BC concentrations were determined by converting the time-resolved light attenuation to BC mass concentration at 650 nm and characterized by a specific mean mass attenuation coefficient as described in (Popovicheva et al. 2017). The calibration parameter for the BC mass quantification was derived during parallel long-term measurements against an AE33 aethalometer (Magee Scientific) that operates at the same three wavelengths.

PM mass concentration with the diameter of aerosol particles smaller than 10 μm (PM10) and aerosol gas precursors were measured at the automatic station for air pollution monitoring with 20-minute resolution operated by the "Mosecomonitoring" State Environmental Protection Agency at the MO MSU. In particular, for the PM10 measurements, the TEOM 1400a instrument (Thermo Environmental Instruments Inc./USA) has been applied. The description of other instrumentation can be found at the Mosecomonitoring site (http://mosecom.ru).

Standard meteorological observations (temperature, relative humidity, pressure, precipitation, wind speed, and wind direction) were taken from the automated Vaisala weather station with 1-minute resolution. Radiative measurements included global shortwave irradiance (less 4 μm) and ultraviolet (UV) irradiance over 300-380nm spectral interval. Global shortwave irradiance (Q) was obtained as a sum of horizontal direct (by the M-3 actinometer) and diffuse (by the M-10 pyranometer with a shadow ring) radiation components, that provided the best Q estimates. The measurements of UV irradiance were fulfilled by the UV-A-T Kipp&Zonen pyranometer calibrated for measuring global UV radiation over the 300-380nm spectral range (Q380) during the Second International UV Filter Radiometer Calibration Campaign UVC-II GAW regional UV calibration center at

PMOD/WRC in Davos, Switzerland (http://projects.pmodwrc.ch/bb2017/project.php). All data were collected in the database with 1-hour resolution. In some cases, we also analyzed instantaneous aerosol measurements. Figure 1 presents a view of the main instrumentation used in the experiment and the picture of MO MSU location.

During the period of the experimental studies the modelling of aerosol was carried out with the help of the COSMO-ART (Vogel et al. 2010; Vil'fand et al. 2017) model with a 7 km grid. The COSMO-ART model simulates chemical transformations of gaseous substances, taking into account for the aerosol chemistry. Chemical processes in the atmosphere are represented by 172 reactions. COSMO-Ru7 was used as initial and boundary conditions for meteorological simulations. The data from Global Land Cover 2000 project were used as land use input parameters. The TNO (Netherlands Organization for Applied Scientific Research) inventory data were utilized to specify anthropogenic emissions of polluting substances. We fulfilled the numerical experiments with different TNO emissions for 2010 and for the 2003-2007 inventory periods. Their spatial distribution for the aerosol gas-precursors emissions for April and May is shown in Fig. 2. It is clearly seen that the latest TNO2010 inventory data are much smaller than the old one. The main experiments in this study were fulfilled with the new TNO2010 emissions. However, some tests were also made with the old 2003-2007 TNO. We should note that only urban aerosol component was significant among other modelling aerosol components. Hence, in

our estimations, the simulated aerosol can be attributed as an urban aerosol. The 24-48-hour COSMO-ART model forecast was analyzed to have enough time for aerosol generation. Mainly we studied surface BC concentration, PM2.5 and AOD550 as well as the important aerosol gas precursors.

RESULTS

The description of weather and optical conditions during the experiment

The AeroRadCity-2018 experiment covered the period from April 1st to 31th of May 2018. During this period monthly mean air temperature was about 8.4^{0}C in April and 16.7^{0}C – in May, relative humidity comprised 54% and 51%, and precipitation - 34 and 45 mm, respectively. Their comparisons showed higher air temperature (+2-3^{0}C), and lower level of relative humidity (10%) and precipitation (7-10 mm) than climatological values over the 1954-2013 period (Chubarova et al. 2014).

Table 1 presents the statistics on the main gaseous and aerosol parameters in the atmosphere of Moscow during the experiment. One can see that AOD at 500 nm (AOD500) was 0.07-0.09 lower than typical AOD for Moscow for these months, while the PM10 concentrations (0.025 mgm^{-3}) were similar to climatological values (0.022 mgm^{-3}) during spring (Chubarova et al. 2014). On average, in Moscow, PM10 was found to be around 0.035 mgm^{-3} that is comparable with their level at European megacities (around 0.020-0.030 mg/m^3) and lower than in Asian megacities (0.05-0.1 mg/m^3) (Climate of Moscow.., 2017;
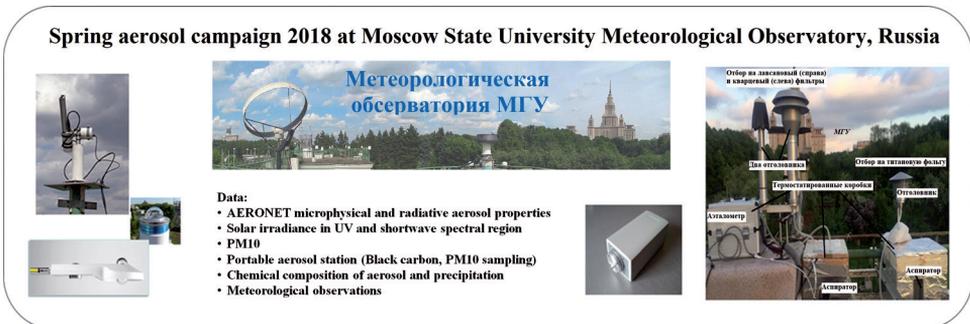
Fig. 1. Main instrumentation used in the AeroRadCity experiment and the picture of MO MSU
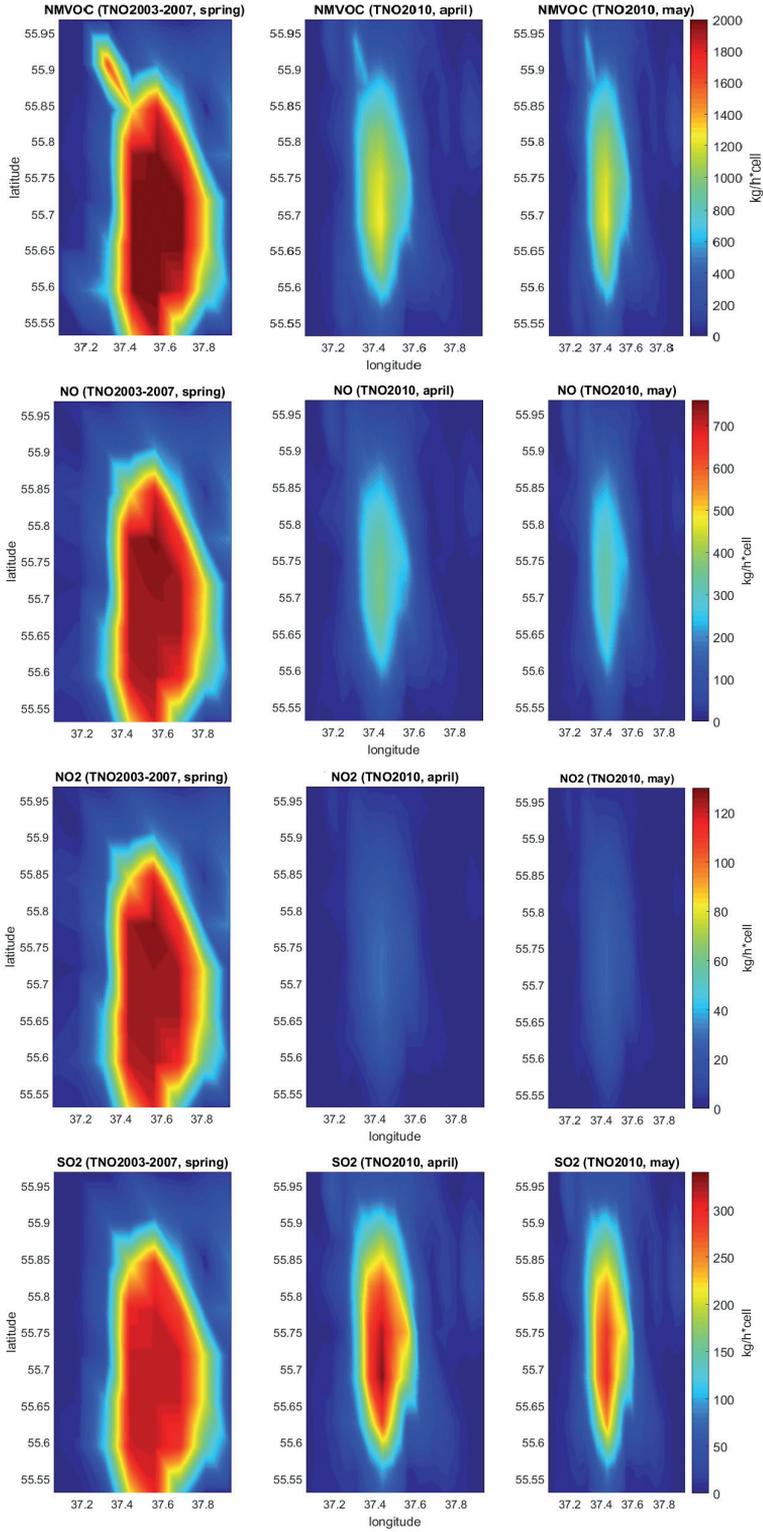
Fig. 2. Emissions of gas-precursors according to the TNO 2010 and the TNO 2003-2007 inventory datasets

Table 1. Characteristics of gaseous and aerosol parameters in the atmosphere of Moscow during the period of the AeroRadCity experiment. April-May, 2018

	Average	50% quantile	Confidence intervals at P=95%	Minimum	Maximum	N case
AOD500	0.14	0.11	0.01	0.06	0.5	194
AOD_{coarse}/AOD, %	37.6	37.1	1.4	9.5	72.8	182
BC*, μgm^{-3}	1.16	0.9	0.07	0.01	8.1	712
PM10, mgm^{-3}	0.025	0.022	0.001	0.001	0.167	1458
BC/PM10*, %	5	4.43	0.27	0.06	61.8	708
SO_2, mgm^{-3}	0.003	0.003	0.0002	0	0.043	1440
NO, mgm^{-3}	0.044	0.032	0.002	0.008	0.33	1440
NO_2, mgm^{-3}	0.037	0.029	0.001	0.008	0.151	1440
CHx, mgm^{-3}	1.45	1.41	0.006	1.32	3.09	1390
CO, mgm^{-3}	0.23	0.2	0.007	0.11	1.31	1440
Angstrom exponent	1.17	1.18	0.031	0.35	1.56	194
Water vapor content, cm	1.22	1.17	0.066	0.35	2.33	194
SSA675	0.86	0.85	0.046	0.81	0.95	7
ASYM675	0.626	0.645	0.051	0.546	0.677	7
Ozone, DU	356.94	353.28	4.63	314.58	440.42	97

Note: statistics were obtained using hourly mean data for ground-based measurements (from initial time step of 20 minute) and direct sun photometer retrievals (with AERONET standard time step setup). Different case number is due to the absence of AERONET measurements in cloudy weather and restrictions on evaluation of SSA and ASYM parameters. Ozone was obtained from OMI satellite data.
*- averaging period from 19 of April to 23 of May 2019

Cheng et al. 2016; The Mosecomonitoring Report 2017). The mean BC concentrations (1.16 $mkgm^{-3}$) were similar to the typical BC for the Moscow region (1.1-1.3 $mkgm^{-3}$) according to (Koepke et al. 1997). However, in (Kopeikin et al. 2018) the Moscow BC concentration was found to be 3 times higher over the highways and central polluted area of Moscow. According to (Emilenko et al. 2018), by the end of 20 century the BC concentration reached 7 $mkgm^{-3}$ in the polluted urban areas. The average 5% BC/PM10 ratio obtained during the experiment was at the upper limit, which typically was smaller than 5%. Its ratio is higher (around 12%) in South America, parts of Africa, Europe, South East Asia, and Oceania due to anthropogenic influence, associated in some cases with biomass burning (IPCC 2007). On average, we can summarize that the analyzed period was characterized by lower total AOD and typical for urban background conditions levels of the surface BC and PM concentrations. The detailed analysis of BC in Moscow for spring conditions 2018 can be found in (Popovicheva et al. 2020).

In order to resolve the effects of aerosol advection and urban aerosol formation processes, the entire period of the AeroRadCity experiment was divided into 12 synoptic sub-periods with quasi-homogeneous atmospheric circulation and meteorological conditions with similar air mass advection according to the detailed analysis of synoptic conditions and 24-hour backward trajectories analysis. Since the concentrations of aerosol and gas composition of the atmosphere were also largely determined by the turbulent conditions in the boundary layer, in addition, the integral quantitative parameter of the intensity of the particle dispersion (IPD) was used in the analysis. The method of its calculation is described in (Kuznetsova et al. 2014). The intensity of air dispersion is classified from 1 to 3 using a number of characteristics including wind speed over 925-850 hPa layer (approximately 1-1.5 km), the type of atmospheric circulation, stratification of the atmosphere and precipitation conditions. For example, when the IPD=1, the atmospheric conditions are characterized by low wind speed, stable stratification, the absence of precipitation, that provides favorable conditions for the pollution accumulation. On contrary, high values of IPD=3 refers to unstable temperature stratification, high wind speed and possible intense precipitation in the zone of the atmospheric front, providing the atmosphere cleaning.

Fig. 3 presents the average values of several columnar and ground-based aerosol characteristics as well as the IPD indices for the 12 sub-periods during the experiment. One can see that the average IPD index is higher than 2 for all sub-periods, that indicates a rather rare frequency of unfavorable meteorological conditions. However, during the two periods –– April 11-16 and May 13-17 we observed statistically significant smaller IPD values due to the prevalence of conditions with stable stratifications and low wind speed in the boundary layer at the elevated atmospheric pressure. One can see that during these periods we have elevated levels of both surface and columnar aerosol including BC component. Note, that during the period with low IPD index the coarse/total aerosol ratio is getting smaller possibly due to the favorable processes of additional accumulation of fine aerosol mode in urban conditions (see Fig. 3). However, during the April 30-May 5 sub-period elevated aerosol values occurred in conditions with a high intensity of particle dispersion. This happened due to air advection from the South-West with elevated levels of aerosol and biomass burning aerosol loading from agricultural fires during the May 1st holiday period.
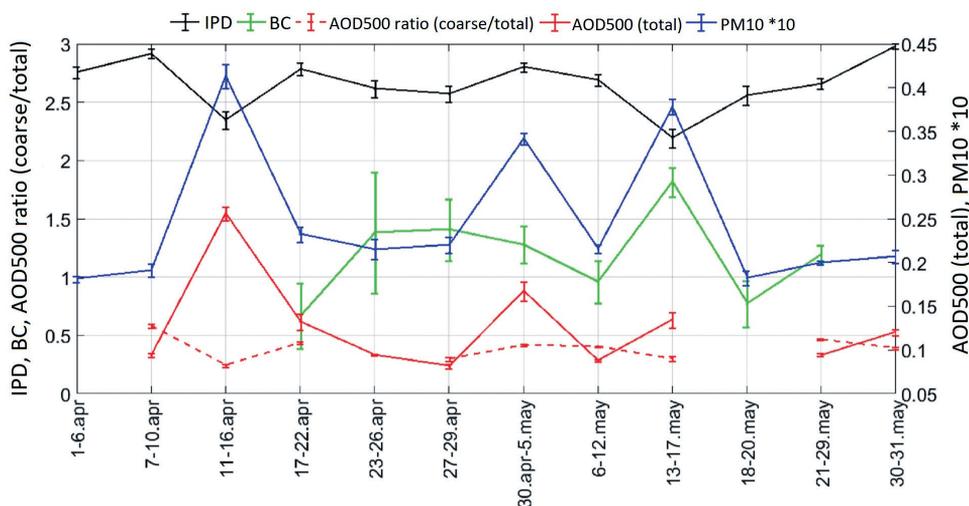
Fig. 3. Average values of AOD at 500 nm, coarse/total aerosol AOD ratio, PM_{10} (mgm^{-3}) and BC ($mkgm^{-3}$) concentrations as well as the index of intensity of particle dispersion (IPD) over the sub-periods of the AeroRadCity experiment

The relationship between different aerosol and gas aerosol precursors

The dependence of columnar AOD500 on PM_{10} and BC values for different classes of the intensity of pollutant dispersion is shown in Fig. 4. One can see that for the dependence of AOD500 versus PM10 (Fig. 4 A, B, C) the two types of relationships with a bifurcation point around PM10=0.04 mgm^{-3} are observed. At high surface PM10 concentrations usually there is an increase in AOD500, but in conditions with IPD=1, low AOD500 can be also observed. This happens due to the conditions of very stable stratification of the atmosphere with accumulation of urban secondary generated aerosol particles near the surface. That means that in such conditions if we analyze the climate effects, even the effective generation of aerosol near the surface will not play any role for radiation and, hence, temperature changes. However, when the AOD500 growth is observed due to the process of the advection from the regions with

elevated columnar aerosol loading the stable stratification (i.e. low IPD index=1) does not play a vital role. On average, we have a statistically significant dependence of AOD500 changes on PM10 for total and fine AOD500 mode (R^2=0.4 in both cases), while no dependence is obtained for coarse mode aerosol (Fig. 4C), since the coarse mode is mainly located near the surface due to larger mass of the particles.

There is no statistically significant AOD dependence on BC concentrations. However, we can see some small sub-visible bifurcation point for total AOD500 at BC=1.5 mkgm^{-3}. Since the size of the BC sample is not large and is smaller than for other components, the studies should be continued before making conclusions.

In order to understand the efficiency of PM_{10} generation, we made comparisons of surface BC dependencies on PM concentration. The increase in PM10 due to BC was obtained according to both the model and experimental
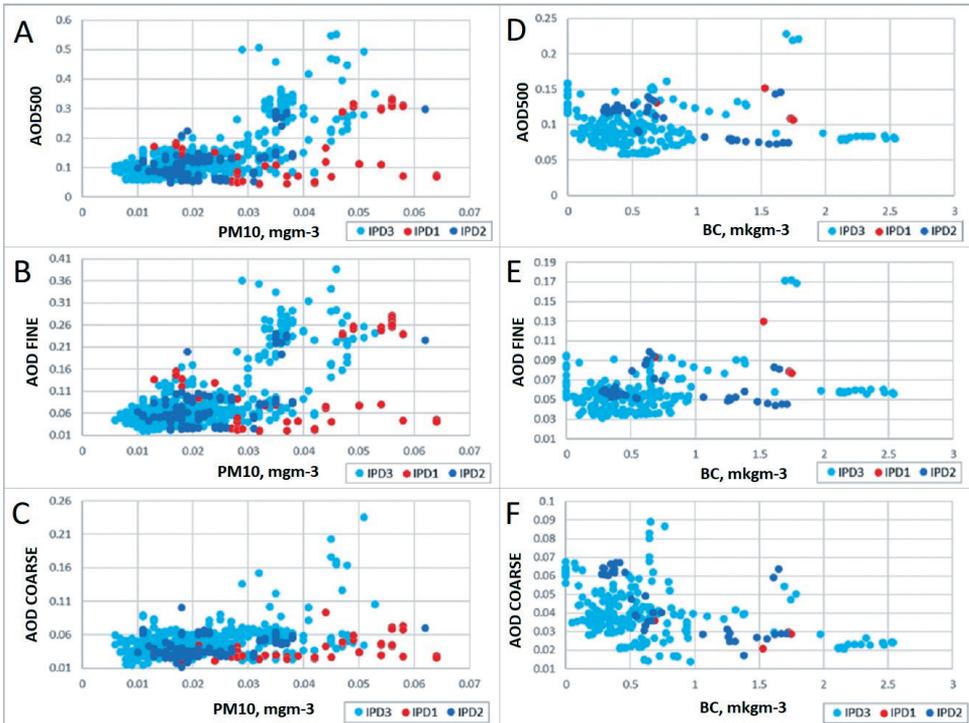
Fig. 4. Columnar AOD500 and AOD500 fine and coarse modes versus PM10 (left panel) and BC (right panel), for different classes of intensity of pollutant dispersion (IPD)

datasets (Fig. 5 A, D). There is also a high correlation between modelled BC and SO_2 concentrations (Fig. 5E). However, according to the measurements, the real SO2 concentrations are much lower and no dependence is seen (see Fig. 5B). This difference can be explained by the overestimation of TNO SO_2 emissions in Moscow. The main source of SO_2 is coal fuel in power plants which is not usually used in Moscow. A high correlation between BC and NO_2 concentrations obtained both in model and experiment demonstrated similar sources of emissions from diesel fuel in motor vehicle transport (Fig. 5 C, F).

Radiative effects of aerosol

In order to reveal the sensitivity of solar irradiance to aerosol, we analyzed the dependence of ultraviolet and global shortwave irradiance on aerosol optical thickness for clear sky conditions. To exclude the solar angle dependence and to evaluate the aerosol effects, radiation was normalized on the corresponding values in the molecular atmosphere. We added the analysis for the UV spectral region 300-380 nm with the effective wavelength at 345 nm, since it is more sensitive to the effects of aerosol and urban gas absorption and at this wavelength, is not practically sensitive to ozone. However, we made the account
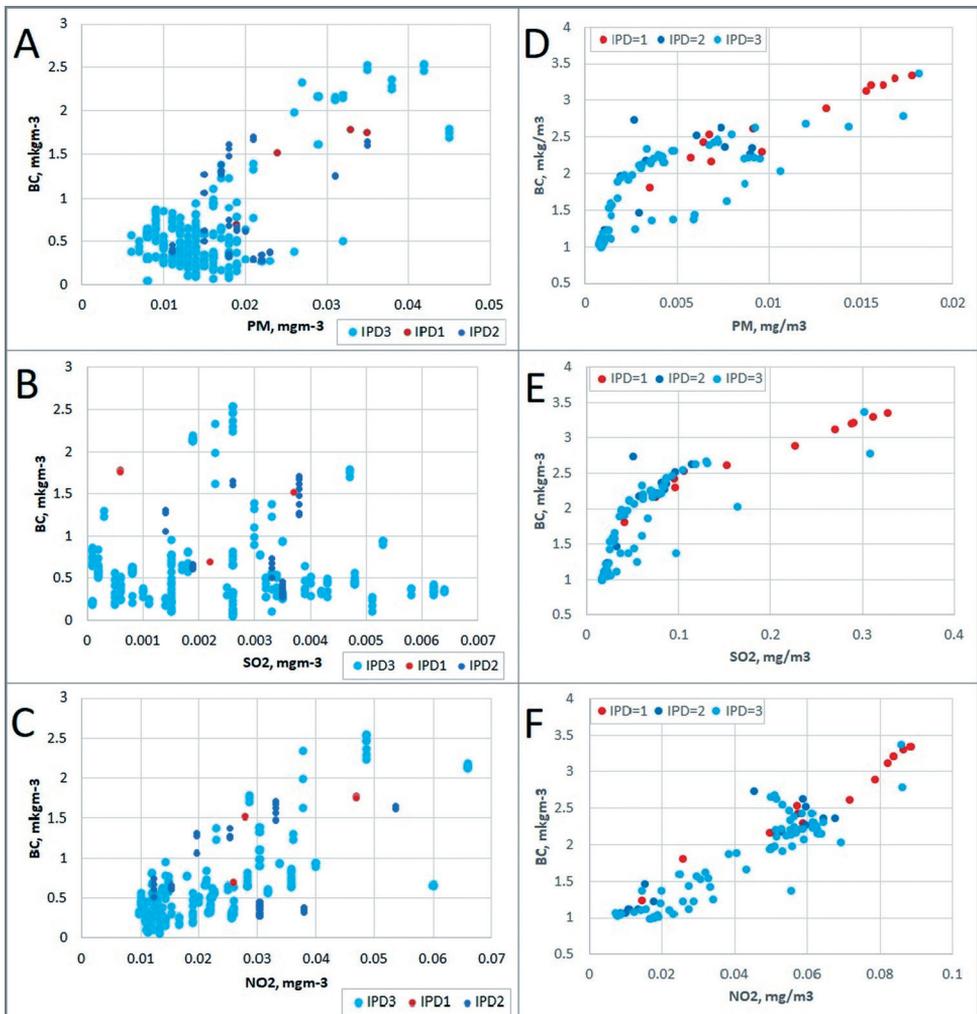
Fig. 5. The BC concentrations versus PM$_{10}$ at different IPD conditions according to measurements (left panel) and COSMO-ART modelling (right panel)

for ozone for UV irradiance according to OMI satellite dataset, which is of few percents, and to water vapor content for shortwave irradiance according to the standard AERONET retrievals. Figure 6 presents the dependence of normalized global shortwave and UV irradiance Qaer/Qmol, % on AOD according to observations and simulations using radiative transfer (RT) DISORT model with different single scattering albedo (SSA). One can see a pronounced dependence with up to 30% loss for UV irradiance and 15% for shortwave irradiance. However, this strong attenuation, especially for UV irradiance, was not reproduced by the RT modelling. When dividing the dataset into morning (before 13:00) and daytime (after 13:00) samples, all low observed values were found in the daytime sample. This result may be due to the fact that the MO MSU is a fairly "clean" site located far from the sources of local pollutant emissions, which are mainly observed at highways and near local points of pollution. In the morning, convective mixing is very weak, so the pollutants are near the earth's surface and do not affect irradiance, while

in the afternoon the convection increases and the polluted air with stronger absorption reaches higher levels affecting even urban background sites. We should mention that AERONET data provide all aerosol properties for visible and near infrared range but no retrievals on single scattering albedo are available for UV spectral region, where these effects are most strong. In addition to black carbon, there can be other types of urban aerosol, i.e., organic carbon aerosols, which have effective absorption in UV (Kirchstetter et al. 2004; Kazadzis et al. 2012). For example, during forest fires in 2010, we have a dramatic decrease in UV irradiance due to high emissions of organic aerosol matter (Chubarova et al. 2012). In addition, we examined the dependence of the SSA retrievals in a visible part of the spectrum on the BC/PM ratio according to our observations. However, due to lack of statistics we were not able to find any dependence, which had been obtained in the previous work (Kozlov et al. 2008).

For different sub-periods, where clear sky conditions were observed, we evaluated
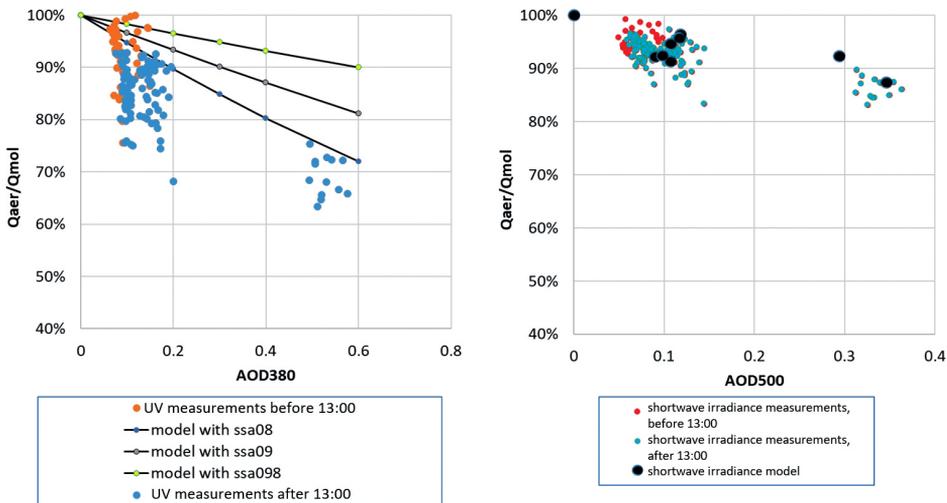
Fig. 6. The dependence of normalized UV (left) and shortwave (right) irradiance (Qaer/ Qmol, %) on aerosol optical depth according to observations and radiative transfer DISORT model. Clear sky conditions

Note. The UV model values were simulated taking into account for the ozone using the OMI satellite data. For shortwave irradiance we accounted for the same water vapor content which was inferred from AERONET standard retrievals. All values were corrected to mean solar-earth distance. The measurements during the first part of the day before 13:00 are shown by orange (left panel) and red (right panel) dots

aerosol radiation forcing effects (RFE) at the top (TOA) of the atmosphere. The RFE is determined following the equation:

$$RFE_{TOA} = - (F_{net,a,TOA} \downarrow\uparrow - F_{net,o,TOA} \downarrow\uparrow) \quad (1)$$

where $F_{net,a}$ and $Fn_{et,o}$ are the net radiation at TOA with and without aerosols, respectively.

Fig. 7 presents RFE at TOA and columnar aerosol characteristics (AOD at 500 nm, single scattering albedo (SSA at 675nm) and aerosol factor of asymmetry (ASYM at 675nm) for different sub-periods in clear sky conditions. The RFE is negative for all periods that provides a cooling effect. It varies from -18 Wm^{-2} during 11-16 April, 2018 to -4 Wm^{-2} during May 6-12, 2018 period due to a substantial decrease in AOD and the conditions with slightly absorbing aerosol (SSA is higher 0.8 for all cases). We also should mention that due to prevalence of smaller aerosol particles we have a smaller factor of asymmetry which can lead to additional cooling effect. Our previous studies we also demonstrated the decrease in surface temperature due to such kind of aerosol is about -0.1…-0.2^{0}C (Chubarova et al, 2018).

Urban aerosol effects over Moscow domain area

We also analyzed, how the modelled urban PM concentrations contribute to the difference in AOD values on the example of Moscow and Zvenigorod (Moscow suburb, background conditions) sites. The Zvenigorod site is located 55 km to the west of Moscow in the upwind direction. This point was chosen since long-term AERONET measurements have been in operation there at the Zvenigorod Scientific Station of Institute of Atmospheric Physics RAS. The comparisons were made for 4 days (15/04, 3/05, 8/05 and 9/05) with different meteorological conditions, when we have large AOD statistics from measurements.

Fig. 8 shows the difference in AOD550 and in PM concentrations between Moscow and Zvenigorod only due to urban aerosol generation for different meteorological regimes according to the COSMO-ART modelling. One can see that according to model results, we have a substantial increase in AOD550 up to 0.05 due to an urban component with an increase in urban PM. No dependence on IPD regimes is seen. The comparison
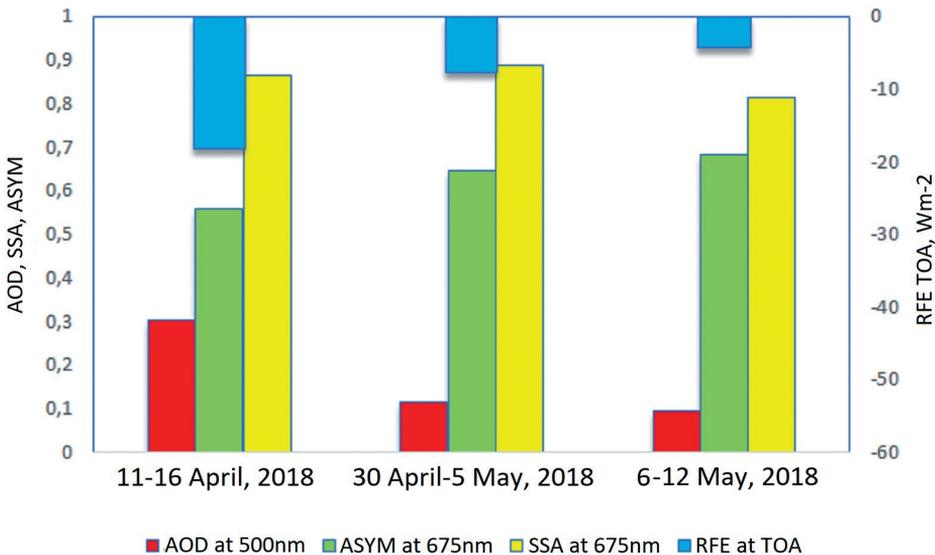
Fig. 7. Aerosol radiative forcing effect (RFE) at the top of the atmosphere and aerosol characteristics (aerosol optical thickness – AOD, ASYM – factor of asymmetry, SSA – single scattering albedo) in clear sky conditions

of modelled and experimental data are presented in Fig. 9, where the deltaAOD550 difference is shown between Moscow and Zvenigorod versus observed PM concentration in Moscow for different meteorological conditions. We clearly see the effects of stable IPD=1 regime on positive urban bias in the observed AOD550. In other IPD regimes, experimental data show both positive and negative differences in AOD550 due to variations in natural aerosol advection. According to modelled data, we see in all cases the increase in AOD in Moscow since we do not take into account natural aerosol in these experiments. In addition,

we should mention that the level of modelled PM concentrations in Moscow is only of urban origin and, hence, is significantly lower than the observed ones.

The application of different emission inventories provides some differences in AOD550 simulations. We made the estimates for two days (8 and 9 of May, 2018), which have revealed that on May 8th the old TNO2003-2007 inventory provided an overestimation of AOD550 difference between Moscow and Zvenigorod (deltaAOD550$_{model}$= 0.055 against deltaAOD550$_{observ}$=0.03),

Fig. 8. The dependence of difference in AOD550 (delta AOD550) on difference in PM concentrations (delta PM) between Moscow (MOMSU, urban conditions) and Zvenigorod (background Moscow suburb conditions) for different meteorological regimes according to the COSMO-ART modelling
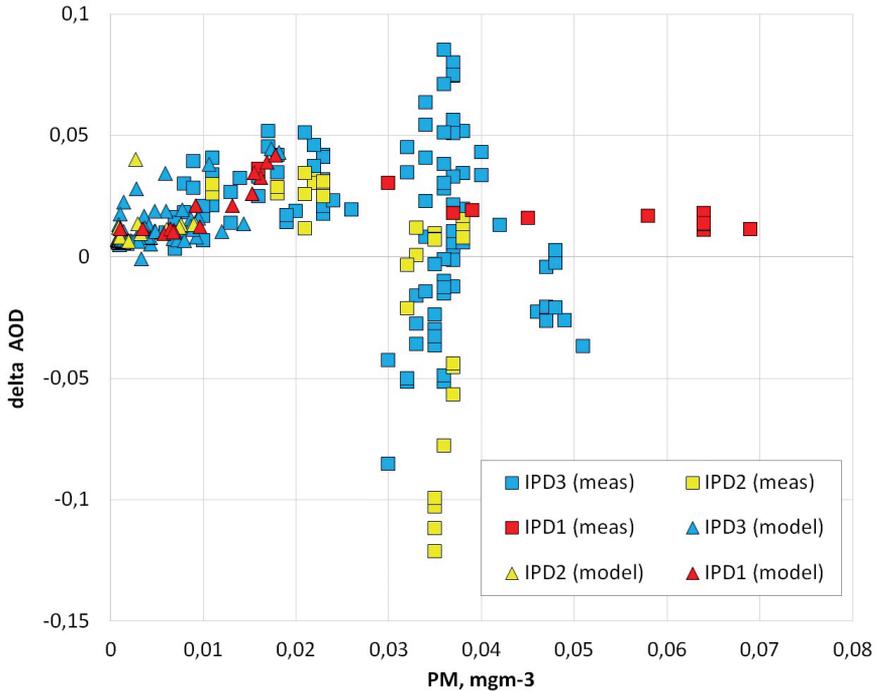
Fig. 9. The difference in AOD550 between Moscow and Zvenigorod (Moscow suburb) as a function of PM concentrations in Moscow for different meteorological IPD regimes according to the COSMO-ART modelling and experimental data

while a new TNO2010 was much closer to measurements (deltaAOD550$_{model}$=0.023). For May 9th the old TNO demonstrated a better agreement (deltaAOD550$_{model}$=0.019 against deltaAOD$_{observ}$=0.017) compared with the new TNO2010 inventory (deltaAOD550$_{model}$=0.007). However, the difference is rather small and lies within the uncertainty of measurements and modelling.

On average, the observed difference between Moscow and Zvenigorod delta AOD550 comprises 0.01 reaching 0.02 at IPD=1 for both the results of modelling and observations (Fig. 10). A smaller range of changes in modelled delta AOD550 is observed since no natural variation of aerosol is taken into account in these numerical COSMO-ART experiments, when mainly urban component of the AOD was calculated with negligible contribution of biogenic aerosol (Fig. 10A). The simulated BC concentration is in agreement with the observed

concentration for urban background conditions over the MO MSU (Fig. 10B). The modeled PM concentrations are much lower than the results obtained from observations since they do not account for natural aerosol components (Fig. 10C). We should emphasize that similar results of about 0.02 for delta AOT500 were obtained in our previous direct comparisons between Moscow and Zvenigorod (Chubarova et al. 2011b). However, in Berlin, much higher difference was obtained when deltaAOD= 0.08 (Li et al. 2018) according to MODIS (MYD04_3K and MYD11_A1) dataset, which might be explained by not full accounting for higher reflectance over the city in the MODIS algorithm. For Warsaw (Poland) conditions, despite much smaller size of the city, the difference is also about 0.02 according to ground based sun photometer measurements (Zawadzka et al. 2013), possibly due to much higher emissions of SO$_2$, which are negligible in Moscow. We should also mention that the level of anthropogenic emission in
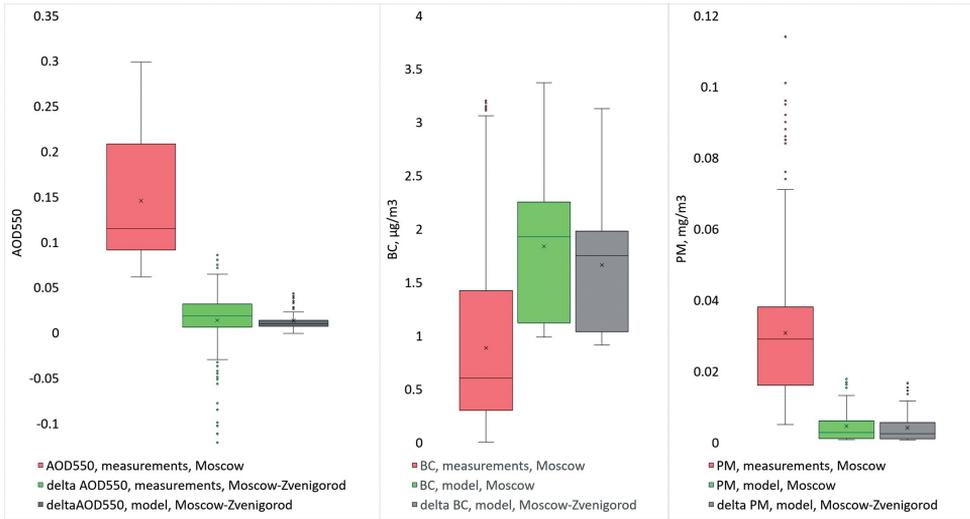
Fig. 10. A box and whisker charts for AOD550(A), BC(B) and PM(C) aerosol characteristics according to measurements and modelling and their difference between Moscow (urban) and Zvenigorod (background conditions). Simulations were made with TNO2010 inventory dataset

Note. Distribution of data is shown in quartiles (interquartile range, IQR), highlighting the mean (sign "X") and outliers (circle signs). The lines extending vertically are error bars. The median (second quartile) is the horizontal line inside the box

Moscow is getting lower during the last decade (Bityukova and Saulskaya, 2017), that causes relatively small AOD increase over the city.

In order to analyze the distribution of urban aerosol over Moscow area, the charts with 7 km grid were made for different days over the whole Moscow district. As an example, Fig. 11 shows the urban aerosol spatial variation for April 15th, 2018 for 10[h] local time. One can see a pronounced high PM concentration over central Moscow with an aerosol plume towards North-East due to

wind predominant direction shown in Fig. 11B. One can see much higher BC concentrations simulated along the highways and over the center of Moscow. The simulated urban AOD550 has also the maximum over the center of Moscow with some plumes over local south-eastern and east areas due to aerosol effective generation over these areas.

DISCUSSION AND CONCLUSIONS

The AeroRadCity-2018 spring experiment, organized at the MO MSU and accompanied by COSMO-ART numerical experiments,

Fig. 11. The spatial distribution of surface BC concentration (A), PM concentrations (B), and AOD550 (C) over Moscow and Moscow suburbs according to the COSMO-ART model simulations. April 15, 7[h] GMT (10h local time)

provided data which joint analysis helps in understanding the processes of aerosol pollution over Moscow megacity. With a large complex of measurements including surface and columnar aerosol characteristics as well as BC concentrations and radiative measurements in different spectral ranges, a detailed study of the observed variations in aerosol and their radiative feedback has been performed.

The analysis of the dependence between AOD500 and PM_{10} has revealed the two types of relationships with a bifurcation point around PM10=0.04 mgm^{-3}. We showed that usually at high PM10 the elevated AOD500 values are observed due to both natural and urban aerosol, but at specific meteorological conditions (IPD=1) the increase in PM can be observed at very low AOD500 level due to conditions of very stable stratification and urban aerosol accumulation near the surface. The detailed analysis of AOD500 relationship with PM_{10} concentrations revealed a positive statistically significant dependence for total and fine AOD500 mode (R^2=0.4 in both cases) while no dependence is obtained for coarse mode aerosol. No statistically significant AOD dependence was obtained with BC concentration and BC/PM10 ratio.

However, high correlation was obtained between PM and BC concentrations according to both model and experimental data, which can be attributed to the important role of BC in PM formation. We also obtain a high correlation between modelled BC and SO_2 concentration, which was not confirmed by measurements with much lower observed SO_2 concentrations. The main source of SO_2 is coal fuel for power plants, which is not usually used in Moscow. Hence, this difference can be explained by the overestimation of TNO2010 inventory on SO_2 emissions in Moscow. A high correlation between BC and NO_2 concentrations demonstrated similar sources of emissions from diesel fuel in motor vehicle transport.

The analysis of radiative effects of aerosol has revealed up to 30% loss for UV irradiance and 15% for shortwave irradiance at high AOD500 in Moscow. However, this strong attenuation, especially for UV irradiance, was not reproduced by RT modelling. We show that situations with strong attenuation relate to the daytime sample, which can be explained by additional effects of more effective afternoon convection at higher level affecting solar irradiance due to increasing absorption. However, the revealed dependence should be studied more on larger statistics at different meteorological conditions. We also obtained a negative radiative forcing effect at TOA for clear sky conditions which lead to the cooling of the atmosphere and earth surface. The significant decrease in its absolute values from -18 Wm^{-2} to -4 Wm^{-2} is explained by the decrease in AOD500 and, to some extent, by aerosol factor of asymmetry due to decrease in aerosol particle size.

On average, the modelled and observed difference in AOD550 during the period of experiment was about 0.01, but in some days deltaAOD550 may increase up to 0.05. We have shown that the generation of urban aerosol is more favorable in conditions with IPD=1, when from both measurements and modelling we obtained deltaAOD550 of about 0.02. The modelled BC concentrations were in agreement with the observed data, however, the PM concentrations were much lower due to not accounting for natural aerosol contribution.

ACKNOWLEDGEMENTS

Natalia E. Chubarova, Elizaveta E. Androsova et al.   AEROSOL AND ITS RADIATIVE EFFECTS ...

04|2019

GES

129

REFERENCES

Bityukova V.R., Saulskaya T.D. (2017). Changes of the anthropogenic impact of Moscow industrial zones during the recent decades. Vestnik Moskovskogo Unviersiteta, Seriya Geografiya, 3, pp. 24-33. (In Russian with English summary)

Cheng Z., Luo L., Wang S., Wang Y., Sharma S., Shimadera H., Wang X., Bressi M., de Miranda R.M., Jiang J., Zhou W., Fajardo O., Yan N., and Hao J. (2016). Status and characteristics of ambient PM2.5 pollution in global megacities. Environment International, vol. 89-90, pp. 212-221. DOI:10.1016/j.envint.2016.02.003.

Chubarova N., Smirnov A., Holben B.N. (2011a). Aerosol properties in Moscow according to 10 years of AERONET measurements at the Meteorological Observatory of Moscow State University. Geography, Environment, Sustainability, vol. 4, № 1, pp. 19-32.

Chubarova N. Y., Sviridenkov M.A., Smirnov A., and Holben B.N. (2011b). Assessments of urban aerosol pollution in Moscow and its radiative effects. Atmospheric Measurement Techniques, vol. 4, № 2, pp. 367–378. DOI:10.5194/amt-4-367-2011.

Chubarova N., Nezval' Ye, Sviridenkov I., Smirnov A., and Slutsker I. (2012). Smoke aerosol and its radiative effects during extreme fire event over Central Russia in summer 2010. Atmospheric Measurement Techniques, vol. 5, pp. 557-568. DOI:10.5194/amt-5-557-2012.

Chubarova N., Belikov I., Gorbarenko E., Eremina I., Zhdanova E.Y., Korneva I., Konstantinov P., Lokoshchenko M., Skorokhod A., and Shilovtseva O. (2014). Climatic and environmental characteristics of Moscow megalopolis according to the data of the Moscow State University Meteorological Observatory over 60 years. Russian Meteorology and Hydrology, vol. 39, pp. 602-613. DOI:10.3103/S1068373914090052.

Chubarova N., Poliukhov A., and Gorlova I. (2016). Long-term variability of aerosol optical thickness in eastern Europe over 2001–2014 according to the measurements at the Moscow MSU MO AERONET site with additional cloud and NO2 correction. Atmospheric Measurement Techniques, vol. 9, № 2., pp. 313–334. DOI:10.5194/amt-9-313-2016.

Chubarova N., Poliukhov A., Shatunova M., Rivin G., Becker R., and Kinne S. (2018). Clear-sky radiative and temperature effects of different aerosol climatologies in the Cosmo model. Geography, Environment, Sustainability, vol. 11, № 1, pp. 74-84. DOI:10.24057/2071-9388-2018-11-1-74-84.

Climate of Moscow in global warming conditions (2017). Edited by Kislov A.V. Moscow: Moscow University Press (in Russian).

Dubovik O. and King M.D. (2000). A flexible inversion algorithm for retrieval of aerosol optical properties from sun and sky radiance measurements. J. Geophys. Res., vol. 105, № D16, pp. 20673-20696. DOI:10.1029/2000JD900282.

Emilenko A.C., Geng-Chen W., Kopeikin V.M., and Isakov A.A. (2018). Urban and regional classes of aerosol taking Beijing and Moscow as examples. Proc. SPIE 10833, 24th International Symposium on Atmospheric and Ocean Optics: Atmospheric Physics, 108334T. DOI:10.1117/12.2504379.

Golitsyn G.S., Grechko E.I., Wang G., Wang P., Dzhola A.V., Emilenko A.S., Kopeikin V.M., Rakitin V.S., Safronov A.N., and Fokeeva E.V. (2015). Studying the pollution of Moscow and Beijing atmospheres with carbon monoxide and aerosol. Izvestiya, Atmospheric and Oceanic Physics, vol. 51, № 1, pp. 1-11. DOI:10.1134/S0001433815010041.

Gubanova D.P., Belikov I.B., Elansky N.F., Skorokhod A.I., and Chubarova N.E. (2018). Variations in PM 2.5 Surface Concentration in Moscow according to Observations at MSU Meteorological Observatory. Atmospheric and Oceanic Optics, vol. 31, pp. 290-299. DOI:10.1134/S1024856018030065.

Holben B.N., Eck T.F., Slutsker I., Tanre D., Buis J.P., Setzer A., Vermote E., Reagan J.A., Kaufman Y.J., Nakajima T., Lavenu F., Jankowiak I., and Smirnov A. (1998). AERONET – A federated instrument network and data archive for aerosol characterization. Remote Sensing of Environment, vol. 66, № 1, pp. 1-16. DOI:10.1016/S0034-4257(98)00031-5.

IPCC (2007): Climate Change 2007: The Physical Science Basis. Contribution of Working Group I to the Fourth Assessment Report of the Intergovernmental Panel on Climate Change. Solomon S., Qin D., Manning M., Chen Z., Marquis M., Averyt K.B., Tignor M., and Miller H.L. (eds.) Cambridge University Press, Cambridge, United Kingdom and New York, NY, USA, 996 pp.

IPCC (2013): Climate Change 2013: The Physical Science Basis. Contribution of Working Group I to the Fifth Assessment Report of the Intergovernmental Panel on Climate Change. Stocker T.F., Qin D., Plattner G.-K., Tignor M., Allen S.K., Boschung J., Nauels A., Xia Y., Bex V., and Midgley P.M. (eds.) Cambridge University Press, Cambridge, UK and New York, NY, USA, 1535 pp.

Kazadzis S., Amiridis V., Kouremeti N. (2013). The Effect of Aerosol Absorption in Solar UV Radiation. In: Helmis C., Nastos P. (eds.) Advances in Meteorology, Climatology and Atmospheric Physics. Springer Atmospheric Sciences. Springer, Berlin, Heidelberg, pp. 1041-1047. DOI:10.1007/978-3-642-29172-2.

Kirchstetter T.W., Novakov T., and Hobbs P.V. (2004). Evidence that the spectral dependence of light absorption by aerosols is affected by organic carbon. J.Geophys.Res., vol. 109, № D21208, pp. 1-12. DOI:10.1029/2004JD004999.

Koepke P., Hess M., Schult I., and Shettle E.P. (1997). Global Aerosol Data Set. Report No. 243, Max-Planck-Institut für Meteorologie, Hamburg.

Kopeikin V.M., Emilenko A.S., Isakov A.A., Loskutova O.V., and Ponomareva T.Ya. (2018). Variations in soot and submicron aerosols in the Moscow region in 2014-2016. Atmospheric and Ocean Optics, vol. 31, № 1, pp. 5-10 (in Russian).

Kozlov V.S., Panchenko M.V., and Yausheva E.P. (2008). Mass fraction of Black Carbon in submicron aerosol as an indicator of influence of smokes from remote forest fires in Siberia. Atmospheric Environment, vol. 42, №. 11, pp. 2611-2620.

Kozlov V.S., Panchenko M.V. Pol'kin V.V., and Terpugova S.A. (2016). Technique for determination of the single scattering albedo of submicron aerosol in the approximation of lognormal size distribution of black carbon. Proc. SPIE 10035, 22nd International Symposium on Atmospheric and Ocean Optics: Atmospheric Physics, DOI: 10.1117/12.2247992

Kuznetsova I., Shalygina I., Nakhaev M., et al. (2014). Unfavorable meteorological factors for air quality Russian Hydrometeocenter Proceedings, vol. 351, pp. 154-172 (in Russian).

Li H., Meier F., Lee X., Chakraborty T., Liu J., Schaap M., Sodoudi S. (2018). Interaction between urban heat island and urban pollution island during summer in Berlin. Science of The Total Environment, vol. 636, pp. 818-828. DOI:10.1016/j.scitotenv.2018.04.254

Mosecomonitoring, 2017 (2016). Environment report in Moscow city. Ed. Kulbachevsky A.O., 363 (in Russian).

O'Neill N.T., Dubovik O., Eck T.F. (2001). Modified Ångström exponent for the characterization of submicrometer aerosols. App. Opt., vol. 40, № 15, pp. 2368-2374. DOI:10.1364/AO.40.002368.

Popovicheva O., Ivanov A., Sitnikov N., Volpert E. (2020). Black carbon in spring aerosols of Moscow urban background. DOI: DOI-10.24057/2071-9388-2019-90. 2020.

Rivin G.S., Rozinkina I.A., Vil'fand R.M., et al. (2015). The COSMO-Ru system of nonhydrostatic mesoscale short-range weather forecasting of the Hydrometcenter of Russia: The second stage of implementation and development. Russian Meteorology and Hydrology, vol. 40, № 6, pp. 400-410. DOI:10.3103/S1068373915060060.

Tegen I., Hollrig P., Chin M., Fung I., Jacob D., and Penner J. (1997). Contribution of different aerosol species to the global aerosol extinction optical thickness: Estimates from model results. J. Geophys. Res., vol. 102, pp. 23895-23915. DOI:10.1029/97JD01864.

Vil'fand R.M., Kirsanov A.A., Revokatova A.P., Rivin G.S., Surkova G.V. (2017), Forecasting the Transport and Transformation of Atmospheric Pollutants with the COSMO-ART Model. Russian Meteorology and Hydrology, vol. 42, № 5, pp. 292–298. DOI:10.3103/S106837391705003X.

Vogel B., Vogel H., Bäumer D., Bangert M., Lundgren K., Rinke R., and Stanelle T. (2009). The comprehensive model system COSMO-ART – Radiative impact of aerosol on the state of the atmosphere on the regional scale. Atmos. Chem. Phys., vol. 9, pp. 8661–8680. DOI:10.5194/acp-9-8661-2009.

Vogel B., Bäumer D., et al. (2010). COSMO-ART: Aerosols and Reactive Trace Gases within the COSMO Model. In: Baklanov A., Mahura A., Sokhi R. (eds.) Integrated Systems of Meso-meteorological and Chemical Transport Models, Springer, pp. 75-80.

Zawadzka O., Markowicz K. M., Pietruczuk A., Zielinski T., and Jaroslawski J. (2013). Impact of urban pollution emitted in Warsaw on aerosol properties. Atmos. Environ., vol. 69, pp. 15–28. DOI:10.1016/j.atmosenv.2012.11.065.

Physikalisch-Meteorologisches Observatorium Davos World Radiation Center (2017). Project, World Calibration Center – Ultraviolet. [online] Available at: http://projects.pmodwrc.ch/bb2017/project.php [Accessed 19 Jun. 2019].

World Health Organization (2019). Ambient (outdoor) air quality and health. [online] Available at: http://www.who.int/mediacentre/factsheets/fs313/en/ [Accessed 19 Jun. 2019].